Reexamination of the Depth Error in XBT Data

Reexamination of the Depth Error in XBT Data

KIMIO HANAWA AND YASUSHI YOSHIKAWA

Department of Geophysics, Tohoku University, Sendai, Japan

(Manuscript received 7 August 1990, in final form 27 November 1990)

ABSTRACT

By using the accumulated datasets of CTD–XBT comparison experiments since 1985, the depth errors for both T-7 and T-6 probes were reexamined. All the XBT probes used here were manufactured by the Tsurumi-Seiki Company, Limited, Japan. The same method as that of Hanawa and Yoritaka was adopted for the detection of depth error. The empirical depth–time equation for T-7 probes newly obtained from an average of all datasets was very similar to that by Hanawa and Yoritaka: depth difference between the corrected and uncorrected data was about 25 m at 800 m. The new equation for T-6 probes based on a single dataset also showed that the depth difference between the corrected and uncorrected data was greater than 10 m at 500 m. It was confirmed that the free-fall velocity estimated by the XBT manufacturer considerably underestimates the actual velocity for both T-7 and T-6 probes.

1. Introduction

An expendable bathythermograph (XBT) measurement is very convenient and suitable for rapid surveys and monitoring of the subsurface temperature structure. Since the procedure for XBT measurements is very easy, XBTs have been used extensively by volunteer observing ships. In the Tropical Ocean Global Atmosphere (TOGA) World Ocean Circulation Experiment and (WOCE) projects, extensive XBT measurements from ships of opportunity as well as from research vessels are underway and are being planned. However, several investigators have pointed out that there are systematic errors in XBT temperature profiles compared with those obtained by more accurate devices such as STD and CTD. For example, Flierl and Robinson (1977), Heinmiller et al. (1983), Hanawa and Yoritaka (1987, hereafter HY), and more recently Yoshida et al. (1989) and Singer (1990) reported on the depth error; i.e., error in the computed free-fall velocity of XBT probes. On the other hand, Roemmich and Cornuelle (1987) examined the error in temperature itself.

Among them, HY proposed the new empirical depth–time equation for XBT T-7 probes (760 m) based on a new detection method for estimating depth error. However, they used only a single comparison dataset made at a single site in 1985. Since then, the authors have conducted three comparison experiments for T-7 probes and one for T-6 probes (460 m) with CTDs at different times and in different water masses. The purpose of the present study is to reexamine the depth error in XBT data using these accumulated datasets.

2. Data and procedure of depth-error detection

a. CTD–XBT comparison experiments

Since 1985 the authors have undertaken the CTD–XBT comparison experiments on cruises of the R/V *Hakuho Maru* and the R/V *Tansei Maru,* which belong to the Ocean Research Institute (ORI), University of Tokyo. Table 1 is the summary of comparison experiments. In all comparison experiments, the Neil Brown CTD-IIIb was used, which has been calibrated by the Physical Oceanography group, ORI, University of Tokyo. Those for T-7 probes were conducted four times (datasets A–D), including that reported by HY, and the experiment for T-6 probes was done once (dataset E). All the XBT probes used here were made by the Japanese licensed manufacturer, the Tsurumi-Seiki Company Limited. Except for thermistors that are imported from the Sippican Inc., United States, all parts of XBT probe are manufactured in Japan.

The experimental procedures used were the same as in HY. After stopping the ship, the CTD fish was lowered at a descent rate of about 1 m s^{-1}. When the fish reached about 100–200 m in depth, the XBT probe was launched. Since the XBT T-7 (T-6) probes finish measuring within about 130 s (70 s), the XBT profiles in the deeper part are taken about 10 (6) min earlier than the CTD profiles. For dataset C, XBT measurements were made every 5 min during one CTD cast: at one CTD station, four XBT probes were launched.

Corresponding author address: Dr. Kimio Hanawa, Department of Geophysics, Physical Oceanography Laboratory, Tohoku University, Sendai 980, Japan.

TABLE 1. Summary of CTD–XBT comparison experiments.

Dataset	Probe type	Number of XBTs	Number of CTD stations	Date	Cruise[a]	Experimental sea area
A	T-7	12	12	December 1985	KH-85-5	around 30°N,135°E
B	T-7	7	7	February 1987	KH-87-1	along 15°N line
C	T-7	8	2	September 1987	KT-87-13	east of Japan
D	T-7	10	10	June 1989	KT-89-9	south of Japan
E	T-6	9	9	June 1989	KT-89-9	south of Japan

Dataset	XBT data converter used	CTD used
A	handmade (ORI)[b]	Neil Brown IIIb[c]
B	handmade (ORI)	Neil Brown IIIb
C	Z-60-II[d]	Neil Brown IIIb
D	Z-60-II	Neil Brown IIIb
E	Z-60-II	Neil Brown IIIb

[a] KH and KT are the cruises of the R/Vs *Hakuho Maru* and *Tansei Maru,* respectively.
[b] See Kitagawa et al. (1981).
[c] Neil Brown Company, Limited.
[d] Murayama-Denki Company, Limited.

Figure 1 shows the locations where the five CTD–XBT comparison experiments were conducted, and Fig. 2 shows the CTD temperature profiles obtained in those comparison experiments. Datasets A and D for T-7 probes, and the dataset E for T-6 probes (the same cruise as D) were taken south of Japan in the northwestern part of the North Pacific subtropical gyre. Dataset B is from the northern part of the North Equatorial Current and dataset C is from the water between the North Pacific subtropical and subpolar gyres: the

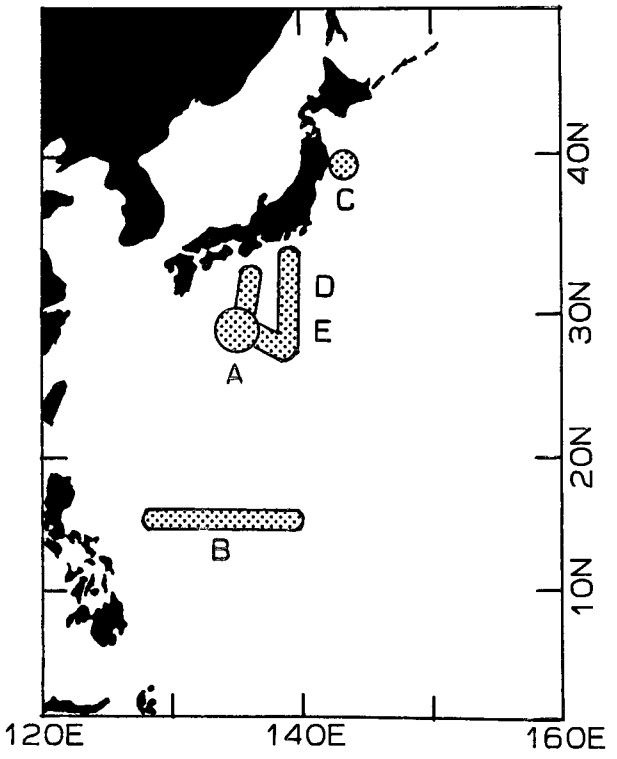

FIG. 1. Locations where CTD–XBT comparison experiments were conducted. Dataset E for T-6 probes was obtained from the same cruise as dataset D for T-7 probes. See Table 1.

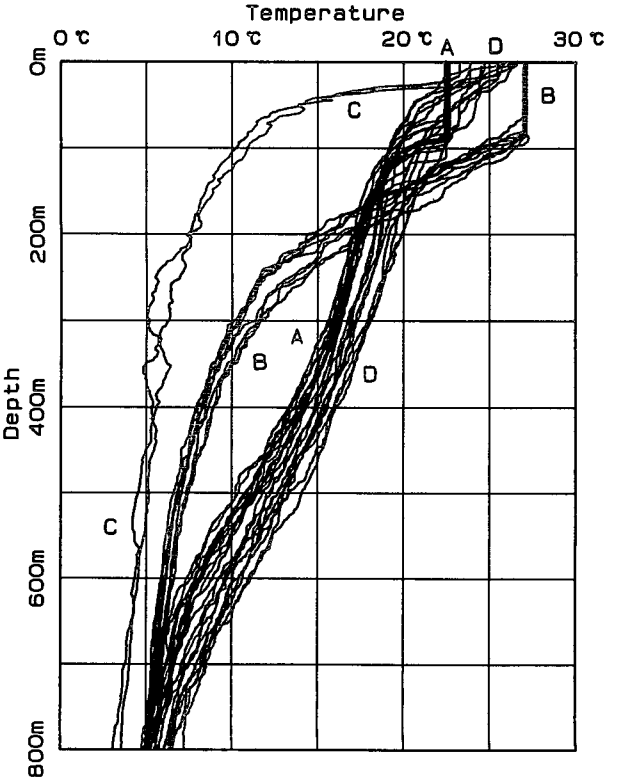

FIG. 2. All CTD temperature profiles for the datasets A–D.

Oyashio and Kuroshio confluence area. It is seen that the temperature profiles are very different in each of the water masses.

b. Procedure of the depth-error detection

The data processing used to determine the depth error is almost the same as in HY. First, both XBT and CTD temperature data were resampled at vertical intervals of 1 m: these are regarded as the "raw" data. At this stage, since the CTD measures pressure, the pressure-depth conversion of the CTD data was made by using the following approximate relation as in HY:

$$z_C = 0.993 p_C, \qquad (1)$$

where z_C is the CTD depth in meters and p_C is the CTD pressure in decibars. Here we chose a density of 1.0275, which lies between 300 and 500 m deep to approximate the density of the upper ocean. This is adequate for our purpose.

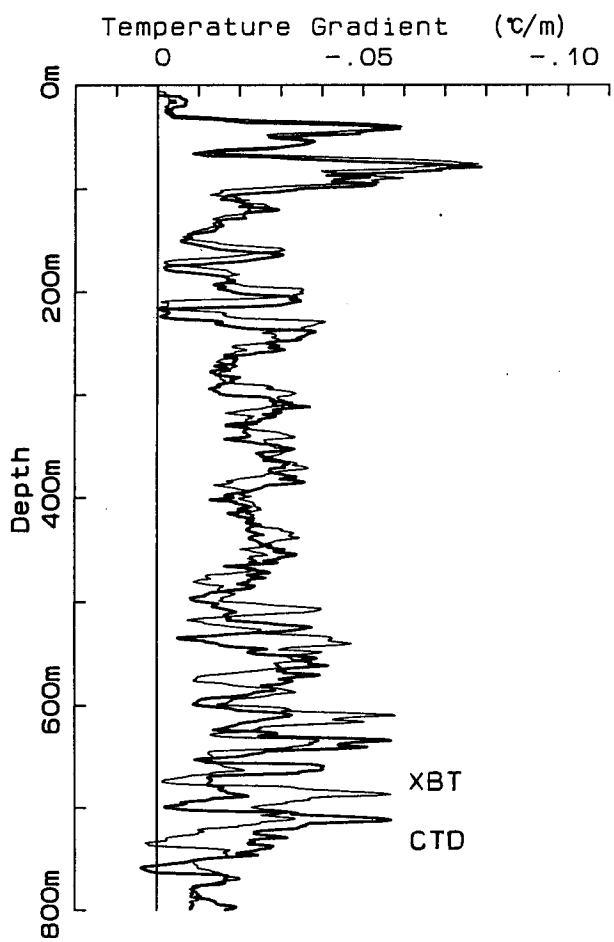

FIG. 3. Example of temperature gradient profiles calculated from the filtered data. Thick and thin lines correspond to CTD and XBT temperature gradients, respectively.

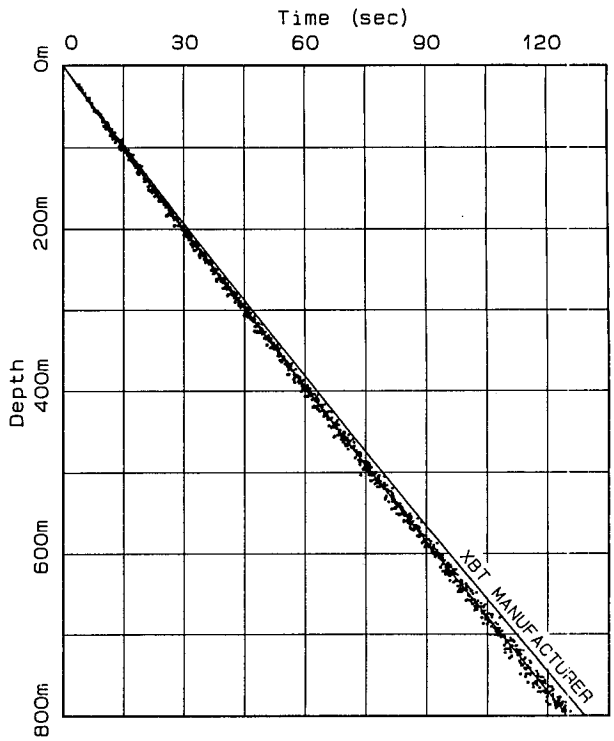

FIG. 4. Scatterplot of the true depths of XBT probes as a function of elapsed time. The full line without dots in the figure denotes the depth–time relationship given by the XBT manufacturer, Eq. (2).

To calculate depth for the XBT probes, the depth–time equation provided by the XBT manufacturer was used at this stage:

$$z_X = 6.472t - 2.160 \times 10^{-3} t^2, \qquad (2)$$

where z_X denotes the XBT depth in meters, and t is the elapsed time in seconds from the time when the XBT probe hits the sea surface.

Next, a simple running average, i.e., box-car filter with 11 points (spacing 10 m of CTD data), was applied to the raw data in the present study, although HY adopted a low-pass filter having a cutoff scale of 30 m and a full-power scale of 60 m. From these filtered temperature profiles, the temperature gradients were calculated. Figure 3 shows an example of CTD and XBT temperature gradient profiles.

Then, the depths of maximum and minimum values of the gradients were selected as the markers, and the differences between two corresponding markers were determined. Identification of the CTD marker and the corresponding XBT marker was made by eye. As is evident in Fig. 3, the corresponding maxima or minima used as markers are easily recognized. The number of markers was 20–30 points for one XBT profile. At this stage, the markers were selected to provide an even distribution along the entire profile; i.e., 3–5 markers per 100 m for the T-7 probes. As a result, a total of about 1000 markers was used for T-7 probes for all

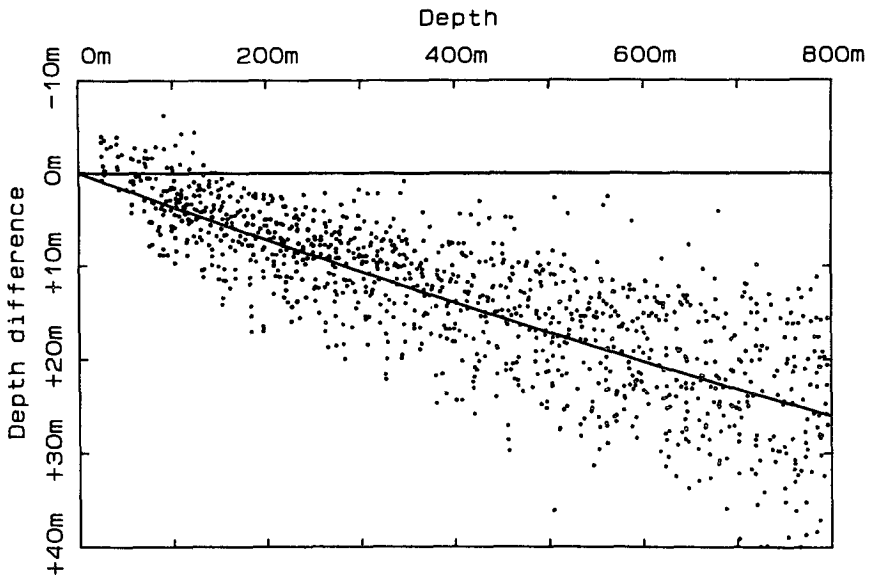

FIG. 5. Scatterplot of depth difference (ordinate) between the true depth of markers and the depth calculated from the equation provided by the XBT manufacturer, Eq. (2) (abscissa). The solid line denotes the depth difference according to the newly estimated empirical depth–time equation (3).

profiles in the present study. Finally, the relation between the elapsed time and the "true" depth, i.e., CTD depth, was examined as described in the next section.

3. Depth–time equation for T-7 probes

a. Depth–time equation for all datasets

Figure 4 shows the scatterplot of the true depths of XBT probes versus elapsed time. The full line without dots in the figure denotes the relationship given by the XBT manufacturer in Eq. (2). In Fig. 5, the ordinate denotes the depth differences between the "true" depths of markers and the depths calculated from Eq. (2), and the abscissa denotes the depth estimated by Eq. (2). Although there is significant scatter in the depth differences for the markers over the entire depth of the profile, this figure clearly shows that an XBT probe falls faster than the fall rate given by the XBT manu-

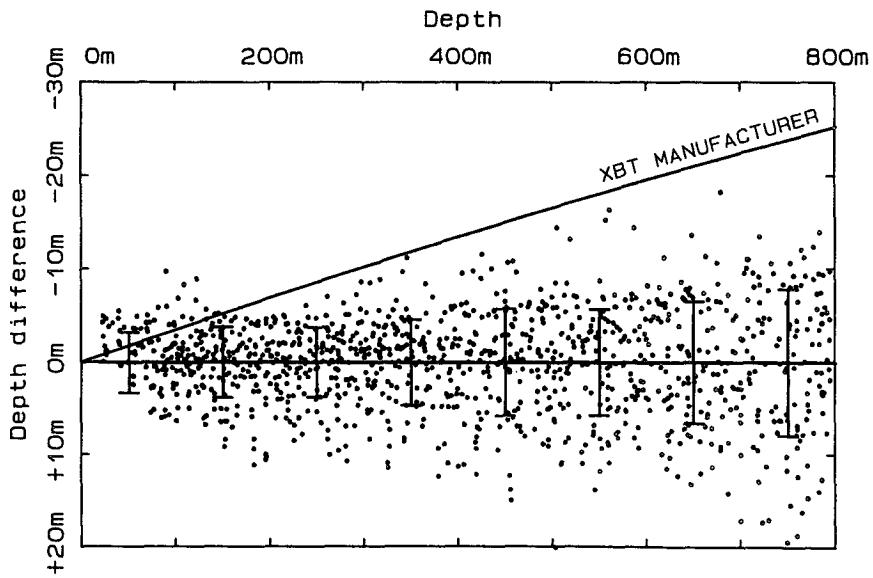

FIG. 6. Scatterplot of the depth difference of the markers to the newly estimated depth–time equation (3). The error bars (plus/minus are standard deviation) are drawn every 100 m.

facturer. The mean value of the depth difference at 700 m is greater than 20 m, which exceeds the accuracy for XBTs stated by XBT manufacturer; i.e., 5 m and/or 2% (Seaver and Kuleshov 1982).

The depth–time equation that best describes all T-7 datasets is estimated by the least-squares method to be

$$z_X = 6.711t - 2.454 \times 10^{-3}t^2, \quad (3)$$

which is also drawn in Figs. 4 and 5 by the solid line surrounded by dots. Here, we assumed that there is no bias component; i.e., no constant term in the depth–time equation. The standard deviation of the XBT markers from surface to 800 m was 5.33 m. This equation is "fortunately" almost the same as that proposed by HY who used only the dataset A in the present study; i.e.,

$$z_X = 6.715t - 2.449 \times 10^{-3}t^2. \quad (4)$$

Figure 6 shows the scatterplot of the depth difference of the markers with the newly estimated equation (3). The standard deviations are drawn every 100 m of true depth in Fig. 6 and show gradual increasing with increasing depth. The standard deviation from the surface to 100 m is not so small and the actual depths of the probes are shallower in this layer than those estimated by both Eqs. (2) and (3). Although there may be several reasons, it is plausible that it takes some time for the probes to reach their terminal velocity of about 6.7 m s^{-1}. Its delay time may depend on the attitude of the probes when they hit the surface, and on the darting of the XBT launcher above the sea surface. In addition, this large scatter may be partly due to the disturbances in the shallower layer caused by the ship screw, the descent of the CTD fish, and due to the existence of large internal waves in the seasonal thermocline.

b. Depth–time equation for the individual datasets

The depth–time equation for each dataset was also determined as follows:

$$\text{Dataset A: } z_X = 6.741t - 2.528 \times 10^{-3}t^2, \quad (5)$$

$$\text{Dataset B: } z_X = 6.652t - 2.030 \times 10^{-3}t^2, \quad (6)$$

$$\text{Dataset C: } z_X = 6.941t - 4.133 \times 10^{-3}t^2, \quad (7)$$

$$\text{Dataset D: } z_X = 6.562t - 1.476 \times 10^{-3}t^2. \quad (8)$$

Reexamination of dataset A used in HY showed that three data were unsuitable for comparison; that is, two XBT data suffered wire stretching (see Fig. 6 in HY) and one CTD profile was very noisy. Therefore, since

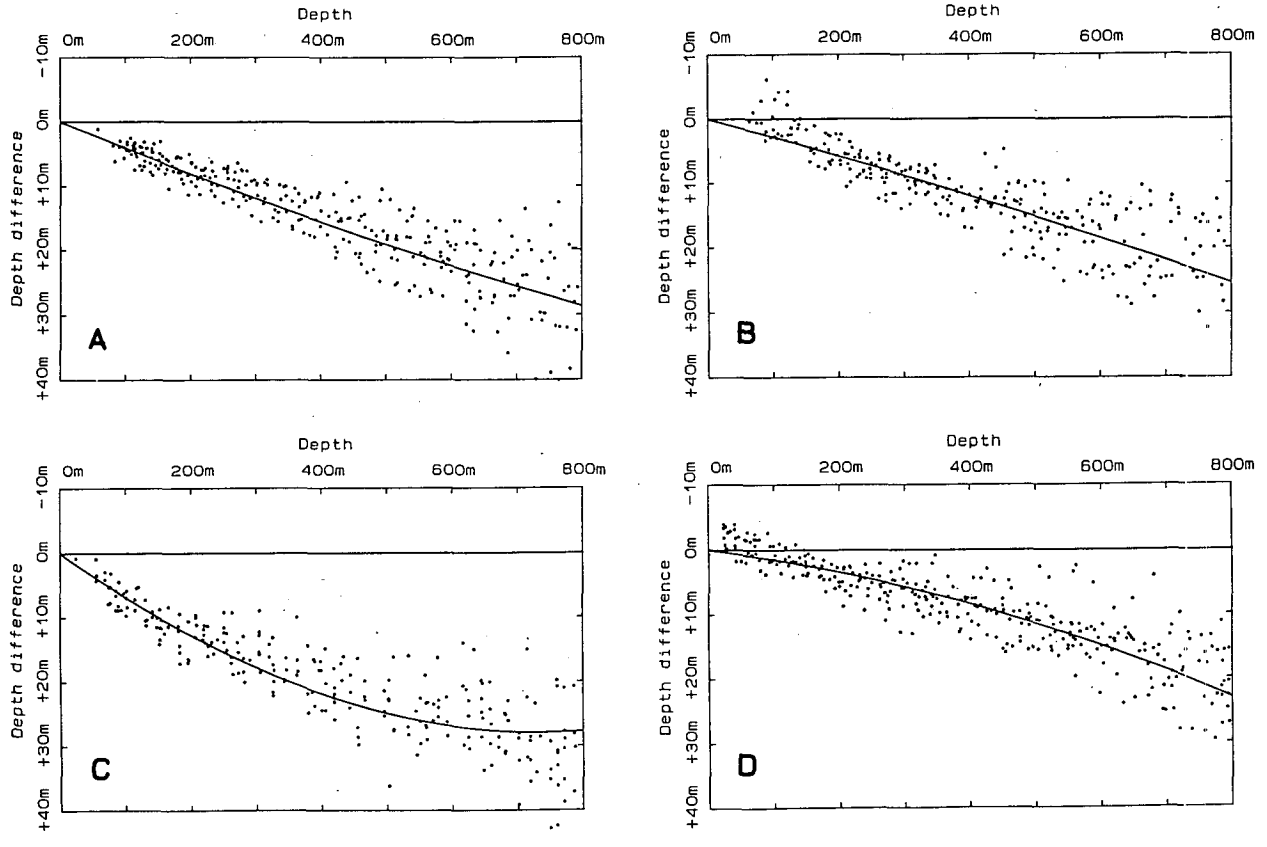

FIG. 7. As in Fig. 5 but for four datasets A through D.

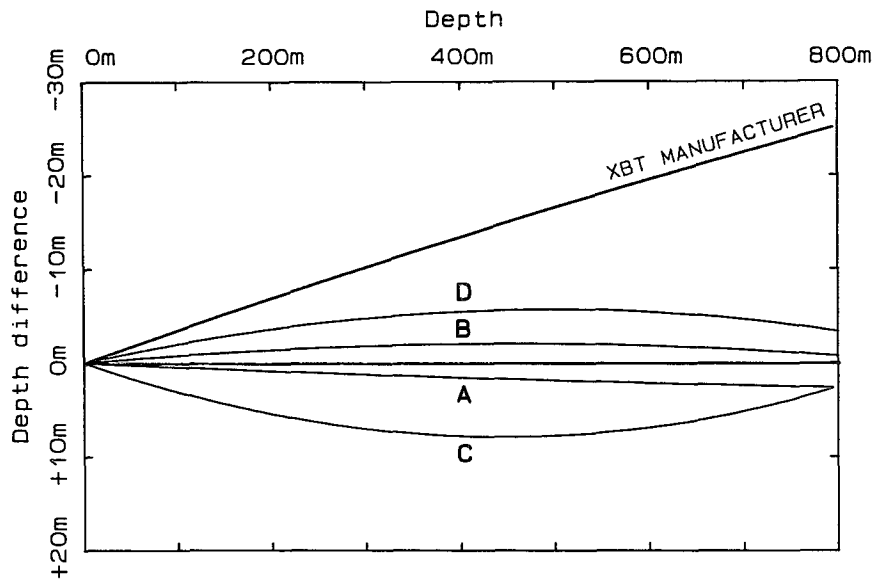

FIG. 8. Difference among four equations individually estimated for four datasets A through D.

three data were discarded in the present analysis, Eq. (5) is slightly different from Eq. (4) by HY.

Figure 7 shows the scatterplot of depth difference as in Fig. 5 but for four datasets A through E. Each panel shows that the markers largely scatter and the standard deviations for depth intervals of 100 m also increase from upper to deeper layers (not shown here). However, an individual dataset seems to have its own systematic tendency. Figure 8 shows the relationship among four equations (5)–(8) to Eq (3). It shows that XBTs of datasets A and C fall faster than Eq. (3), while those of datasets B and D fall slower. Since mean vertical temperature profiles depend on the sites of the comparison experiment as seen in Fig. 2, the difference in the sea water viscosity, i.e., the drag coefficient for the XBT probes, may be a possible explanation for the difference in Eqs. (5)–(8).

Assuming that at low temperatures water has high viscosity, XBTs of datasets B and C suffer higher drag compared with those of datasets A and D, because water temperatures in experimental sites of datasets B and C are relatively lower than those in datasets A and D as seen in Fig. 2. Therefore, it can be expected that XBTs of datasets B and C fall much slower than those of datasets A and D. However, Fig. 8 shows that XBTs of dataset C fall fastest among four datasets, while those of dataset D fall slowest. Those of datasets of A and B fall with velocity between the above two datasets; that is, it is concluded that tendency of XBT fall rate as shown in Fig. 8 cannot be explained from the viewpoint of water viscosity, and we must search for another reason.

Since the XBTs used here were made at different times (different lots), there may be small but systematic changes in shape and weight of the probes. Here, it is very interesting to point out that the relationship between the two constants a and b (positive value), multiplied by t and t^2, respectively, in the depth–time equation, has a quasi-linear relationship as shown in

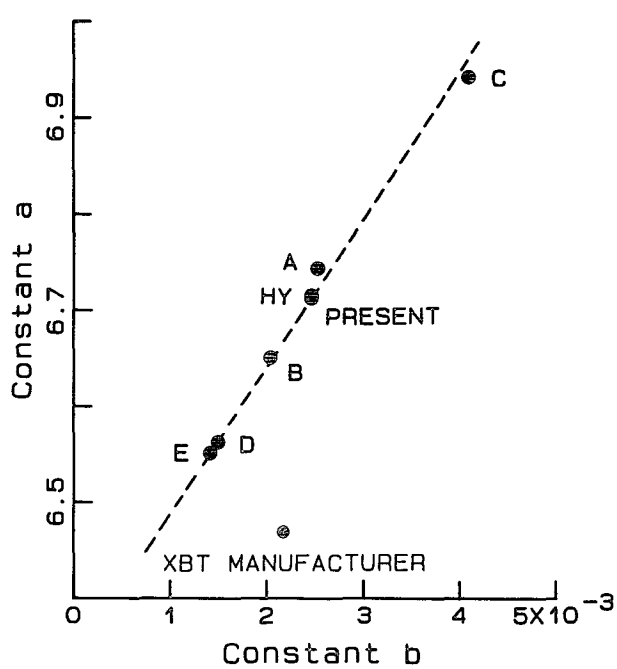

FIG. 9. Relationship between two constants a (ordinate) and b (abscissa), which are multiplied by t and t^2, respectively, in the depth–time equations. Symbols denote datasets. That for T-6 probes (dataset E) is also presented.

Fig. 9. The constant a can be regarded as the free-fall velocity at the initial stage (very close to the terminal velocity), while constant b reflects the temporal rate of velocity due to the reduction of the probe weight by releasing wire.

The most plausible cause, which explains the above relationship between constants a and b, may be attributed to the differences in the enamel thickness used on the probe wire; that is, when the wire is thick in diameter and is thinly coated with enamel, the weight per unit length of wire is heavier and the buoyancy of the whole probe is small compared with the standard one. Therefore, this probe can fall faster at the initial state—i.e., larger constant a—but it becomes slower rapidly because of the faster reduction of the probe weight by the release of heavier wire—i.e., larger b. On the other hand, when the wire is thin in diameter and is thickly coated with enamel, the probe falls slower at first, and keeps its velocity to the later stage because of the situation opposite from the situation described above. This situation will lead to smaller constants a and b.

The Japanese XBT manufacturer (Mr. S. Suzuki, personal communication,) recognizes that it is very difficult to make wire with uniform diameter and enamel coating. Actually, they find that wire weight in water shows largest scatter among the parts of probe. Here, it should be noted that the total weight of the XBT probe is inspected *only in air* by an XBT manufacturer and is adjusted by reeling wire, i.e., wire length.

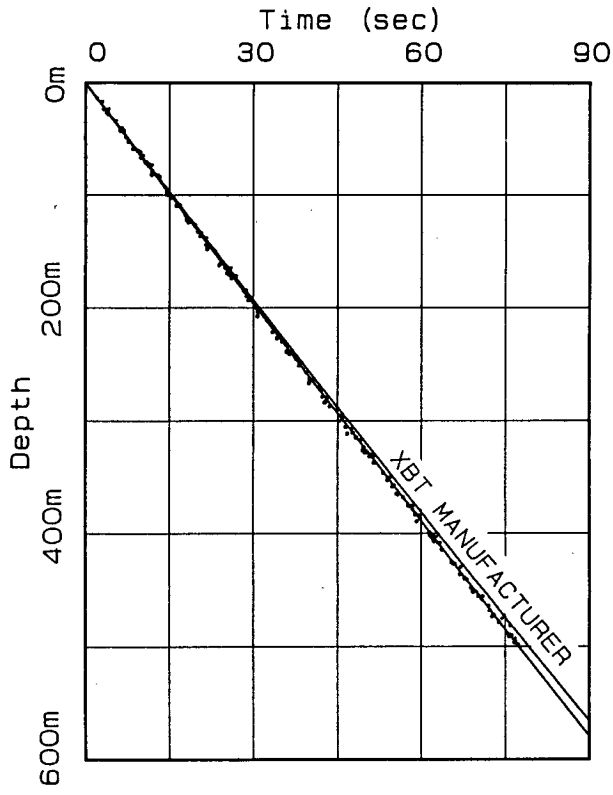

FIG. 10. As in Fig. 4 but for T-6 probes (dataset E).

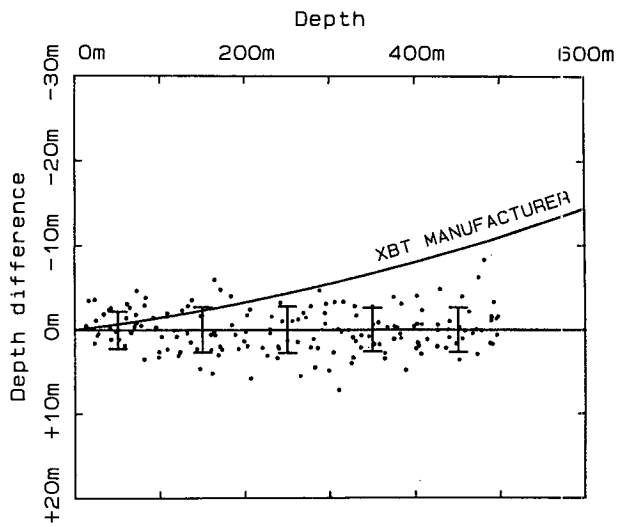

FIG. 11. As in Fig. 6 but for T-6 probes (dataset E).

The above discussion is just qualitative, and quantitative verification must be made by using some physical model. However, its task is beyond the scope of the present study.

4. Depth–time equation for T-6 probes

The depth error was also examined for the XBT T-6 probes (dataset E). Figure 10, as in Fig. 4, shows the relation between the true depths of XBT probes and the elapsed time. This figure also shows that an XBT T-6 probe falls faster than the fall rate given by the XBT manufacturer, as well as the T-7 probe. The mean value of the depth difference at 450 m is about 10 m, which also exceeds the accuracy for XBTs stated by XBT manufacturer. From these data, the following depth–time equation was obtained:

$$z_X = 6.553t - 1.378 \times 10^{-3}t^2. \qquad (9)$$

The scatter of the markers, which is almost independent on depth, is rather small compared with those for T-7 probes as shown in Fig. 11. The mean standard deviation of the markers from surface to 500 m was 2.53 m. Note that constants a and b in Eq. (9) also lie on the line of a quasi-linear relationship between constants a and b for T-7 probes, as shown in Fig. 9. Since dataset E consists of only nine probes, more data for T-6 probes are needed to confirm this equation.

5. Concluding remarks

In the present study, the free-fall velocities of T-7 and T-6 probes were reexamined using data from five CTD–XBT comparison experiments since 1985. Following the method adopted by HY, it was confirmed

that the free-fall velocity estimated by the XBT manufacturer considerably underestimates the actual velocity for the T-7 probes, as was pointed out by HY. The new empirical depth–time equation [Eq. (3)] for T-7 probes obtained by using all the datasets was almost the same as that obtained by HY. However, the empirical equations for individual datasets were different from each other, and seem to have a systematic tendency. A new depth–time equation for T-6 probes was also obtained as Eq. (9).

Since XBTs used here were made by the Japanese licensed manufacturer, it goes without saying that the comprehensive CTD–XBT comparison experiments at different times and in different water masses with XBTs manufactured by all makers would be very useful.

Finally, the authors must comment on the use of the newly estimated equations (3) and (9); that is, although an individual investigator is invited to use the newly estimated equations for individual studies, XBT data sent to the national or international XBT data centers should be those calculated by a single, internationally accepted, equation, i.e., that provided by the XBT manufacturer, Eq. (2). The existence of mixed data in the database must be absolutely avoided.

Acknowledgments. The authors would like to express their sincere thanks to all scientists, the captain, officer and crew in the cruises of KH-85-5, KH-87-1, KT-87-13, and KT-89-9, by the R/Vs *Hakuho Maru* and *Tansei Maru.* Thanks are extended to Mr. S. Suzuki, Tsurumi-Seiki Company, Limited, for his response to the authors' questions and requests. The authors also acknowledge comments by an anonymous reviewer.

This study was made as part of OMLET (Chairman: Prof. Y. Toba), one of the Japanese WCRP activities, which was financially supported by the Japanese Ministry of Education, Science and Culture. The first author (KH) was also financially supported by the Grant-in-Aid for Scientific Research (63460042, 1988–90) of the same ministry.

REFERENCES

Flierl, G., and A. R. Robinson, 1977: XBT measurements of the thermal gradient in the MODE eddy. *J. Phys. Oceanogr.*, **7**, 300–302.

Heinmiller, R. H., C. C. Ebbesmeyer, B. A. Taft, D. B. Olson and O. P. Nikitin, 1983; Systematic errors in expendable bathythermograph (XBT) profiles. *Deep-Sea Res.*, **30**, 1185–1196.

Hanawa, K., and H. Yoritaka, 1987: Detection of systematic errors in XBT data and their correction. *J. Oceanogr. Soc. Japan*, **43**, 68–76.

Kitagawa, S., K. Taira and T. Teramoto, 1981: A digital data logger for the XBT. *La mer*, **19**, 165–170. [Japanese with English abstract and captions.]

Roemmich, D., and B. Cornuelle, 1987: Digitization and calibration of the expendable bathythermograph. *Deep-Sea Res.*, **34**, 299–307.

Seaver, G. A., and A. Kuleshov, 1982: Experimental and analytic error of the expandable bathythermograph. *J. Phys. Oceanogr.*, **12**, 592–600.

Singer, J. J., 1990: On the error observed in electronically digitized T-7 XBT data. *J. Atmos. Oceanic Technol.*, **7**, 603–611.

Yoshida, J., T. Suzuki, H. Sudo and M. Matsuyama, 1989: Corrected of XBT depth error. *J. Tokyo Univ. Fish.*, **76**, 55–63. [Japanese with English abstract and captions.]